Molecular Biology of the Cell
Vol. 21, 739–752, March 1, 2010

Enhanced H2AX Phosphorylation, DNA Replication Fork Arrest, and Cell Death in the Absence of Chk1

Mary E. Gagou, Pedro Zuazua-Villar, and Mark Meuth

Institute for Cancer Studies, School of Medicine and Biomedical Sciences, University of Sheffield, Sheffield, S10 2RX, United Kingdom

Submitted July 27, 2009; Revised December 22, 2009; Accepted December 24, 2009
Monitoring Editor: Jonathan Chernoff

H2AX phosphorylation at serine 139 (γH2AX) is a sensitive indicator of both DNA damage and DNA replication stress. Here we show that γH2AX formation is greatly enhanced in response to replication inhibitors but not ionizing radiation in HCT116 or SW480 cells depleted of Chk1. Although H2AX phosphorylation precedes the induction of apoptosis in such cells, our results suggest that cells containing γH2AX are not committed to death. γH2AX foci in these cells largely colocalize with RPA foci and their formation is dependent upon the essential replication helicase cofactor Cdc45, suggesting that H2AX phosphorylation occurs at sites of stalled forks. However Chk1-depleted cells released from replication inhibitors retain γH2AX foci and do not appear to resume replicative DNA synthesis. BrdU incorporation only occurs in a minority of Chk1-depleted cells containing γH2AX foci after release from thymidine arrest and, in cells incorporating BrdU, DNA synthesis does not occur at sites of γH2AX foci. Furthermore activated ATM and Chk2 persist in these cells. We propose that the γH2AX foci in Chk1-depleted cells may represent sites of persistent replication fork damage or abandonment that are unable to resume DNA synthesis but do not play a direct role in the Chk1 suppressed death pathway.

INTRODUCTION

The orderly and precise replication of cellular DNA is essential to maintain genome stability. Therefore, cells respond to disruptions of DNA replication by protecting the integrity of stalled forks, suppressing the firing of new replication origins, and initiating repair. Considerable evidence has accumulated that the PIK-like kinase Ataxia telangiectasia–mutated and Rad3–related (ATR) and its downstream phosphorylation target Chk1 are crucial for this response (Cimprich and Cortez, 2008). Inhibition of DNA replication in many cell types leads to ssDNA formation that appears to be a result of the continued unwinding of DNA by the helicase complex in the absence of replication progression (Byun *et al.*, 2005). These ssDNA regions become coated with RPA that, in turn, interact with the ATR-interacting protein (ATRIP) and ATR (Zou and Elledge, 2003; Ball *et al.*, 2005). The formation of this complex is necessary for efficient phosphorylation and activation of Chk1 (Zou and Elledge, 2003) although Chk1 also may be phosphorylated by ATR where ATR-ATRIP complex does not bind to RPA (Ball *et al.*, 2005). Activated Chk1 coordinates many of the cellular responses to replication fork stress. More specifically, it prevents the inappropriate firing of late replication origins, abandonment of replication forks, and premature chromosome condensation after disruption of replication (Feijoo *et al.*, 2001; Nghiem *et al.*, 2001; Zachos *et al.*, 2003; Maya-Mendoza *et al.*, 2007). It has also been reported that Chk1 activation is required for homologous recombination (HR)-mediated restart of replication forks stalled by replication inhibitors (Sorensen *et al.*, 2005).

More recently Chk1 has been shown to play a key role in protecting cells from apoptosis in response to many types of DNA damage (Rodriguez and Meuth, 2006; Sidi *et al.*, 2008). p53-deficient tumor cells depleted of Chk1 show an enhanced level of apoptosis in response to ionizing radiation (IR; Sidi *et al.*, 2008). This death pathway is caspase-2–dependent and requires both Ataxia telangiectasia mutated (ATM) and ATR. Chk1 also suppresses apoptosis induced by DNA replication inhibitors. When Chk1 is depleted, replication inhibitors trigger death in S-phase cells in a caspase-3–dependent manner (Rodriguez and Meuth, 2006; Myers *et al.*, 2009). However the death response to replication inhibitors is independent of p53 status (Rodriguez and Meuth, 2006) and does not require ATM or ATR function (Myers *et al.*, 2009). Previous work from our group has shown that apoptosis induced by replication inhibitors in Chk1-depleted cells can be suppressed by depletion of the essential replication helicase cofactor Cdc45 and is enhanced in p21-deficient cells, indicating that events tied to DNA replication integrity or origin firing in the absence of Chk1 may be key to triggering this death response (Rodriguez and Meuth, 2006; Rodriguez *et al.*, 2008). Other reports have indicated that the variant histone core protein H2AX is phosphorylated at serine 139 after treatment with a Chk1 inhibitor, particularly in the presence of agents that inhibit DNA replication (Syljuasen *et al.*, 2005; Ewald *et al.*, 2007). This phosphorylated form of H2AX (called γH2AX) has mostly been studied in association with DSB formation (Rogakou *et al.*, 1998). γH2AX appears within minutes of IR-induced DNA double-strand break (DSB) formation through the action of ATM and DNA-activated protein kinase (DNA-PK) activities (Stiff *et al.*, 2005). γH2AX is distributed over a megabase swath of DNA surrounding a DSB to form γH2AX foci (Rogakou *et al.*, 1999) and plays a key role in the recruitment

This article was published online ahead of print in *MBC in Press* (http://www.molbiolcell.org/cgi/doi/10.1091/mbc.E09–07–0618) on January 6, 2010.

Address correspondence to: Mark Meuth (e-mail: m.meuth@sheffield.ac.uk).

of DNA repair and signaling factors to the site of damage, in some cases through physical interactions with the proteins (Paull *et al.*, 2000; Stucki *et al.*, 2005). H2AX-deficient cells are IR-sensitive, show impaired repair of DSBs, and exhibit chromosome instability (Celeste *et al.*, 2002). γH2AX can also be detected in cells at later stages of apoptosis during DNA fragmentation (Rogakou *et al.*, 2000) and has been reported to be required for this fragmentation but not for caspase-3 activation (Lu *et al.*, 2006).

In the work reported here we investigated the role of H2AX phosphorylation in the Chk1 suppressed apoptotic pathway responding to DNA replication stress. We show an enhanced level of γH2AX in Chk1-depleted cells exposed to replication inhibitors that can persist even when cells are shifted to normal medium. Our data indicate that Chk1-depleted cells retaining γH2AX are less likely to succumb to apoptosis after replication stress although γH2AX does not appear to facilitate the restart of stalled replication forks or reentry into the cell cycle.

MATERIALS AND METHODS

Cell Lines and Cultures

The HCT116 and SW480 human colon cancer cell lines were obtained from American Type Culture Collection (Manassas, VA), and the p21 derivative of HCT116 cell line was provided by Dr. Bert Vogelstein (Johns Hopkins University, Baltimore, MD). The immortalized human fibroblast cell line MRC5 VA was obtained form the CRUK London Laboratories Cell Repository.

Cells were maintained in DMEM supplemented with 10% fetal bovine serum (FBS). For experiments using thymidine, dialyzed FBS was used to remove deoxynucleosides in the serum that might interfere in the response to this agent. Replication inhibitors thymidine and hydroxyurea (HU) were used at a concentration 2 mM. For some experiments cells were irradiated using a CIS IBL 437 Cs-137 irradiator. In some experiments a chemical inhibitor of Chk1 activity (Gö6976, Calbiochem, La Jolla, CA; Kohn *et al.*, 2003) was used at concentrations 0.1 or 1 μM. The inhibitor was added to cell cultures 1 h before treatment with replication inhibitors.

Small Interfering RNA Transfection

The Chk1 small interfering RNA (siRNA) was designed by J. Blackburn and C. Smythe, having the following sequence (sense strand: GAAGCAGUCGCAGUGAAGA). For Cdc45 depletion two different sets of siRNAs were used. The first set (L-003232-00; Dharmacon, Lafayette, CO) consisted of a pool of four small interfering RNA (siRNA) doublexes with the following sense sequences: GUCAAUGUAUACAACGAUAUU, CGUCAGCCAUGGUGAUGUUUU, UCACUCAAAUGAAAUACGUUU, and GCAAAGAGUUCUACGAGGUUU. The second set (HSS112144, HSS112145, and HSS112146; Invitrogen, Paisley, United Kingdom) consisted of a pool of three stealth siRNA doublexes with the following sense sequences: GACGUGGUCUUUGCCACCAUGUCUU, GGCACUCCAGAUGUCAUGCUGUUCU, and GACAGCCUGUGCAACACCAGCUAUA.

Control siRNAs, containing nonspecific sequences that do not have homology in human genome, were provided by Eurogentec (Hythe Southampton, Hampshire, United Kingdom; OR-0030-NEG) or Invitrogen (Stealth siRNA Negative control 12935-400). siRNA and/or Stealth siRNA duplexes were transfected into cells using Lipofectamine 2000 (Invitrogen) according to manufacturer's instructions. The cells were then incubated for 24 h before further treatment.

Cell Cycle Analysis

Cell cycle analysis of floating and adherent cells was performed as described previously (Rodriguez and Meuth, 2006).

Detection of Apoptosis

In Vivo Detection of Caspase-3 Activation versus Cell Cycle. After appropriate treatments, floating and adherent cells (obtained from the medium and a PBS wash or after trypsinization, respectively) were pooled and pelleted by centrifugation. Cell pellets were washed with PBS and assayed for active caspase-3, using the CaspGLOW fluorescein active caspase-3 kit according to the manufacturer's instructions (MBL, Woburn, MA). Cells were then costained with propidium iodide (PI) by resuspension in PBS containing 5 μg/ml PI, 100 μg/ml RNAse A and 0.1% (vol/vol) Triton X-100. After 30-min incubation, stained nuclei were analyzed on a FACsCalibur (BD Biosciences, Franklin Lakes, NJ) using Cell Quest software.

TUNEL Assay. Floating and adherent cells (obtained as described above) were assayed for terminal deoxynucleotidytransferase dUTP nick end labeling (TUNEL), using the APO-BRDU kit according to the manufacturer's instructions (BD PharMingen, San Diego, CA). Stained nuclei were analyzed by flow cytometry.

Flow Cytometric Analysis of γH2AX

Pellets of floating and adherent cells were washed with PBS, fixed in 70% ice-cold ethanol, and stored at −20°C for up to 2 wk. After two washes with PBS, cells were incubated for 15 min on ice in hybridization buffer (PBS containing 0.5% bovine serum albumin [BSA] and 0.25% Triton X-100). After centrifugation, cells were hybridized with an Alexa 488–conjugated rabbit monoclonal anti- γH2AX antibody (Cell Signaling, Beverly, MA; 9719) diluted at a ratio of 1:10 in hybridization buffer, and incubated for 1 h in the dark at room temperature (RT). Cells were then rinsed twice with PBS containing 0.25% Triton X-100 and stained with PI solution (PBS containing 5 μg/ml PI, 100 μg/ml RNAse A) for 30 min before flow cytometry.

Immunofluorescence Analysis

For γH2AX foci staining, cells were grown on glass coverslips, treated as indicated, fixed with 3% buffered paraformaldehyde for 15 min at RT, and permeabilized in PBS containing 0.5% Triton X-100 for 8 min at RT. Cells were then incubated with 1:500 diluted polyclonal anti-γH2AX antibody (Cell Signaling; 2577) for 45 min at RT and detected with a secondary Alexa 488–conjugated goat anti-rabbit IgG (A11008; Molecular Probes, Invitrogen, Eugene, OR). Antibody dilutions and washes after incubations were performed in PBS containing 0.5% BSA and 0.05% Tween 20. Coverslips were finally mounted in Vectashield mounting medium with DAPI (H-1500; Vector Laboratories, Burlingame, CA).

For simultaneous analysis of TUNEL+ cells and γH2AX, cells were cultured, fixed, and permeabilized as described above. Then, the TUNEL assay was performed according to the manufacturer's instructions (ApoAlert DNA Fragmentation Assay Kit; Clontech, A Takara Bio, Palo Alto, CA). At the end of this assay, cells were washed with PBS containing 0.25% Triton X-100 for 5 min at RT and further stained with the anti-γH2AX antibody specified above for 45 min, followed by a 30-min staining with a secondary Alexa 594–conjugated goat anti-rabbit IgG (A110012; Molecular Probes, Invitrogen). For simultaneous detection of γH2AX and the activated form of caspase-3, cells were cultured on glass coverslips and treated with siRNAs and replication inhibitor according to standard procedures. At the end of the treatments, cells washed twice with PBS and incubated with the FITC-conjugated caspase-3 inhibitor DEVD-FMK (CaspGLOW fluorescein active caspase-3 kit; MBL, Woburn, MA), at a dilution of 1:300, at 37°C for 1 h. They were then washed twice with PBS and fixed, permeabilized, and stained for γH2AX as described above.

For double staining of γH2AX with RPA, cells were preextracted with PHEM buffer (45 mM HEPES, pH 6.9, 45 mM PIPES, pH 6.9, 10 mM EGTA, pH 7.0, 5 mM $MgCl_2$) containing 0.1% Triton X-100 and 1 mM PMSF for 1min at RT before being fixed, permeabilized, and stained as described above. For RPA detection, mouse anti-RPA34 (NA19L; Calbiochem) was used at a dilution of 1:500 and detected with a secondary Alexa-594–conjugated goat anti-mouse IgG (A11005; Molecular Probes, Invitrogen).

Immunofluorescence was visualized using a Nikon Eclipse T200 inverted microscope (Melville, NY), equipped with a Hamamatsu Orca ER camera (Bridgewater, NJ) and a 200 W metal arc lamp (Prior Scientific, Cambridge, United Kingdom), with a 100× objective. Images were captured as wide-field acquisitions, analyzed by Volocity 3.6.1 software (Improvision, Coventry, United Kingdom) and further processed with ImageJ software (http://rsbweb.nih.gov/ij/). At least 300 cells were analyzed for each individual experiment, and experiments were repeated twice. In experiments where the fraction of colocalized foci were measured, HCT116 Chk1-depleted cells treated for 6 h with thymidine were used (after longer exposures to thymidine the γH2AX signal becomes considerably diffused). At least 100 cells were analyzed from wide-field acquisition overlays. The colocalization factor was defined as previously described by Sengupta *et al.* (2004): [(fraction of cells having colocalization) × (fraction of foci colocalized per cell)] × 100.

Detection of Bromodeoxyuridine Incorporation

Pulse Labeling. Untreated cells or cells exposed to thymidine were washed thoroughly with thymidine-free medium and cultured in fresh medium containing 10 μM bromodeoxyuridine (BrdU; Sigma-Aldrich) for 1 h. Cells were then harvested directly or left to grow in BrdU-free medium for varying lengths of time before harvest.

BrdU Staining for Flow Cytometric Analysis. Cell pellets were washed with PBS, fixed in 70% ice-cold ethanol, and stored at −20°C for up 2 wk. To denature DNA, fixed cells were resuspended in 2N HCl and incubated for 30 min at RT. After thoroughly washing with PBS, to remove any acid traces, cells were hybridized with a mouse monoclonal anti-BrdU antibody (DakoCytomation, Carpinteria, CA; M0744) diluted at a ratio of 1:50 in PBST (PBS containing 0.1% BSA and 0.2% Tween 20, pH 7.4) and incubated for 20 min at

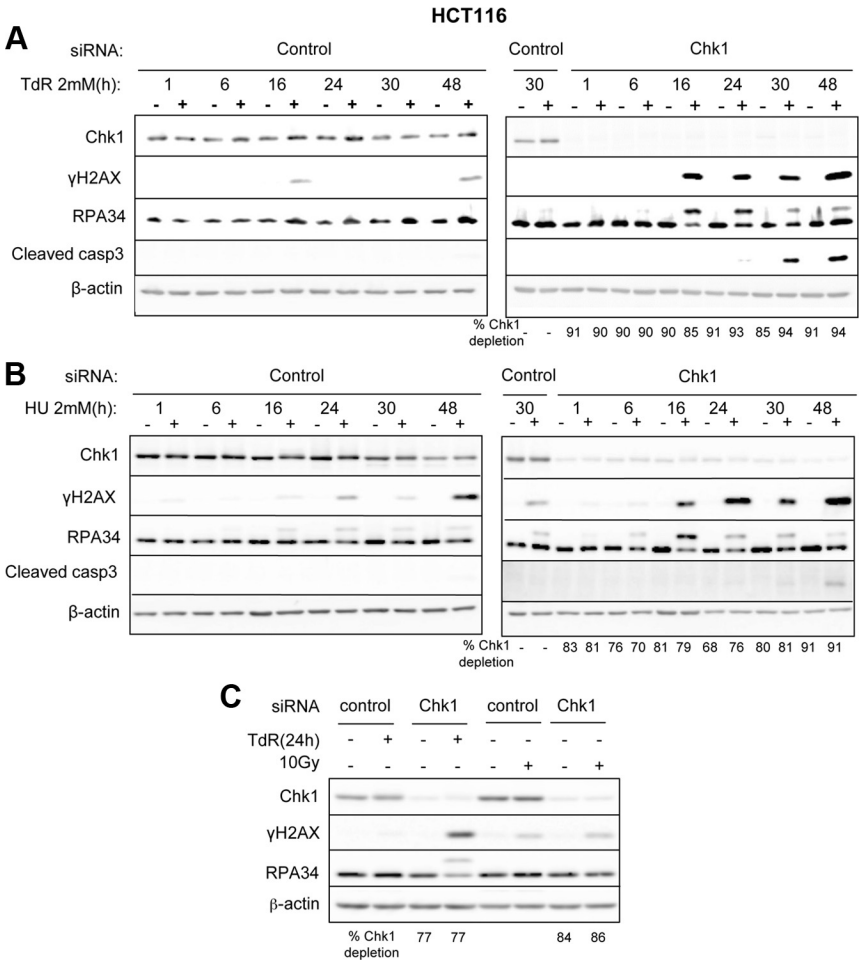

Figure 1. Induction of γH2AX in Chk1-depleted cells upon replication stress coincides with RPA34 hyperphosphorylation and precedes apoptosis. Western blot analysis of γH2AX, RPA34, and cleaved caspase-3 in extracts obtained from HCT116 cells transfected with control or Chk1 siRNAs treated or not treated with 2 mM thymidine (TdR) (A) or 2 mM hydroxyurea (HU; B) for the indicated times. The band showing slower mobility on panel probed with the RPA34 antibody represents hyperphosphorylated forms of the protein. (C) Western blot analysis of γH2AX and RPA34 in extracts obtained from HCT116 cells transfected with control or Chk1 siRNAs after a 24-h treatment with 2 mM thymidine or exposure to 10 Gy of IR. Cells exposed to IR were harvested 1 h after treatment. β-Actin levels are presented as loading controls. The percent depletions of Chk1 for cultures treated with the Chk1 siRNAs are presented. These values were normalized to the β-actin levels loading controls.

RT. Cells were then rinsed with PBS containing 0.2% Tween 20 and incubated with FITC-conjugated rabbit anti-mouse immunoglobulin antibody (DakoCytomation; F0313) diluted at a ratio of 1:10 in PBST. After 20-min incubation at RT in the dark, cells were washed with PBS and stained with PI solution for 30 min before flow cytometry.

BrdU Staining for Microscopic Analysis. Cells were cultured, fixed, and permeabilized according to standard protocol, as described above. Cells were then treated with 100 U/ml DNase (Promega, Madison, WI; M6101) for 30 min at RT. After that, cells were incubated with the above mouse anti-BrdU simultaneously with a rabbit anti-γH2AX antibody (Cell Signaling; 2577), for double labeling with γH2AX, or with a rat anti-RPA34 antibody (Cell Signaling; 2208), for double labeling with RPA34. Primary antibodies were detected with a secondary goat anti-mouse Alexa594 (A11005; Molecular Probes, Invitrogen) and an Alexa 488–conjugated goat anti-rabbit IgG (A11008; Molecular Probes, Invitrogen) or an Alexa 488–conjugated goat anti-rat IgG (A11006; Molecular Probes, Invitrogen).

Protein Extraction and Western Blotting

Whole-cell extracts were prepared and fractionated by SDS-PAGE before being blotted onto nitrocellulose (Whatman Schleicher & Schuell, Dassel, Germany) as described previously (Bolderson *et al.*, 2004). Proteins were detected with the ECL detection system (GE Healthcare, Little Chalfont, Buckinghamshire, United Kingdom) using the following specific antibodies: γH2AX (2577; Cell Signaling), Chk1 (2360; Cell Signaling), β-actin (A-5060; Sigma-Aldrich), RPA34 (NA19L; Calbiochem), cleaved caspase-3 (ab32042; Abcam, Cambridge, United Kingdom), Cdc45 (sc-20685; Santa-Cruz Biotechnology, Santa-Cruz, CA), p21 Waf1/Cip1 (2947; Cell Signaling), phospho-ATM (Ser1981; 2152-1; Epitomics, Burlingame, CA), phospho-Chk2 (Thr68; 2661; Cell Signaling), and phospho-Chk1 (Ser295; 2349; Cell Signaling). Band intensities on the Western blots were quantified by densitometry using the ImageJ software. Relative total Chk1 levels were normalized to corresponding β-actin levels. Subsequently, Chk1 depletion efficiencies are given relative to total Chk1 levels in control untreated cells.

RESULTS

Enhanced γH2AX Formation in Chk1-depleted Cells Treated with Replication Inhibitors Precedes Apoptosis

To determine the effect of Chk1 depletion on the induction of H2AX phosphorylation after DNA replication stress, HCT116 cells treated with control or Chk1 siRNAs were exposed to thymidine or HU for up to 48 h. At various times cell extracts were prepared from these cultures, and γH2AX, RPA34, and active caspase-3 were analyzed by Western blotting. Cells treated with the control siRNA showed a transient induction of γH2AX at 16–24 h after treatment with thymidine or HU (Figure 1, A and B). At later times γH2AX levels decreased before increasing again at ~48 h after treatment with replication inhibitor, most likely in response to DNA fragmentation that occurs in some of the cells (Rogakou *et al.*, 2000). In Chk1-depleted cells this phosphorylation could be detected at about the same time (16 h) but was distinctly stronger and more persistent. γH2AX accumulation coincided with the hyperphosphorylation of RPA34 and occurred well in advance of caspase-3 activation. The high level of γH2AX in Chk1-depleted cells treated with replication inhibitors was not limited to HCT116 as SW480 and MRC5 cells depleted of Chk1 showed a similar induction of γH2AX and RPA34 phosphorylation after thymidine treatment (Supplemental Figure S1, A and B). Additionally enhanced levels of γH2AX and RPA hyperphosphorylation were detected after thymidine exposure of HCT116 cells

treated with a Chk1 inhibitor (Gö6976) that has been shown to mimic the effects of the Chk1 siRNA (Sidi *et al.,* 2008; Beckerman *et al.*, 2009; Supplemental Figure S1C).

The level of γH2AX accumulating in Chk1-depleted cells treated with thymidine was clearly elevated relative to cells exposed to IR (Figure 1C). Interestingly Chk1 status did not affect the level of γH2AX in IR-treated cells and RPA hyperphosphorylation was not detected in any of the cells exposed to IR. The timing of H2AX phosphorylation in control or Chk1-depleted cells exposed to IR was distinctly different from that found in cells treated with replication inhibitors (Supplemental Figure 2A). After a 10-Gy dose of IR, HCT116 cells showed a rapid but transient induction of H2AX phosphorylation detectable as early as 30 min after treatment that persisted up to 2 h.

To further characterize the kinetics of H2AX phosphorylation during replication stress, we used flow cytometry to measure the fraction of HCT116 cells containing γH2AX and DNA content. Consistent with the Western blots presented above, ~8% of HCT116 cells treated with the control siRNA showed γH2AX induction at 16 h after thymidine exposure (Figure 2, A and B). In Chk1-depleted HCT116 cells treated with thymidine a significantly higher proportion of cells showed H2AX phosphorylation (35–60%) at 16–48 h of exposure (Figure 2, A and C). This was not due to the accumulation of cells in S-phase as there was no significant difference in cell cycle distribution in cells treated with control or Chk1 siRNAs (Figure 2, B and C, middle panels).

PI staining revealed that, in the absence of Chk1, γH2AX accumulates in cells at the G1/S border and in S-phase at 16 to 24 h after thymidine treatment (Figure 2C, bottom panel). After longer exposures to thymidine (30 and 48 h), γH2AX appears mainly in S-phase cells, coinciding with the movement of the cell population into S-phase. In contrast, H2AX phosphorylation in control cells was spread throughout all phases of the cell cycle with the greatest density of positive cells in G2/M after 48-h thymidine arrest (Figure 2B, bottom panel).

The above FACS analysis also revealed the accumulation of cells with a subG1 DNA content in Chk1-depleted cultures after 30 h of thymidine treatment (Figure 2, A and C), consistent with the detection of activated caspase-3 at this time in the Western blots (Figure 1A). Because both of these measures of apoptosis occurred much later than γH2AX induction, it seemed unlikely that the H2AX phosphosphorylation observed at early times was a result of the DNA fragmentation that occurs as cells undergo apoptosis (Rogakou *et al.,* 1999). Interestingly only a small proportion (7.9%) of Chk1-depleted cells with a subG1 DNA content had an increased level of γH2AX after a 48-h thymidine treatment (Figure 2C, top panels, UL). To further confirm the late onset of apoptosis, we measured in vivo activation of caspase-3 in a FACS-based assay and TUNEL+ cells under the above conditions of replication stress. The fraction of cells with active caspase-3 showed little change after thymidine treatment of Chk1-depleted cells until 36 h, when a robust increase was detected (Supplemental Figure S3A). There was relatively little increase in the fraction of cells staining for active caspase-3 after treatment with the control siRNA or in cells treated with either siRNA in the absence of thymidine. Similarly there was a significant increase in the fraction of TUNEL+ cells in Chk1-depleted HCT116 cultures treated with thymidine at 48 h (Supplemental Figure S3B). Thus the induction of γH2AX formation significantly preceded the onset of apoptosis.

γH2AX and RPA Foci Colocalize in Chk1-depleted Cells Treated with Thymidine

Given the localization of γH2AX to foci at sites of damage after IR, we next investigated the nuclear organization of γH2AX in Chk1-depleted cells treated with replication inhibitors.

In HCT116 cells treated with the control siRNA, low levels of γH2AX foci (1–10/cell) were detected after 6 h of thymidine treatment, and the fraction of such cells continued to increase through 24 h (Figure 3A and B). Cells with higher levels of foci were less common at all times. In Chk1-depleted cells, varying patterns of nuclear H2AX phosphorylation were detected after thymidine arrest (Figure 3, A and B, Supplemental Figure S4). After a 6-h exposure some cells stained weakly and had few foci (1–10 foci), whereas others had widespread foci (>10/cell) and more intense staining. In addition a small fraction of cells showed diffuse, bright pan-nuclear staining (Figure 3A). This heterogeneity might reflect a difference in staining in cells in early or late S-phase (Cowell *et al.,* 2007). The frequency of cells showing pan-nuclear staining markedly increased after longer exposure times (16 and 24 h) in the absence of Chk1. Cells with >10 foci also increased while those with <10 foci decreased at 24 h. A similar response was seen in HCT116 cells treated with the Chk1 inhibitor Gö6976 (data not shown).

Immunofluorescence analysis was next performed to investigate the relationship between RPA foci that form in Chk1-depleted cells treated with replication inhibitors (Rodriguez *et al.,* 2008) and γH2AX foci. At early times after thymidine treatment when the foci were distinct (6 h, Figure 3B), 92% of cells with RPA and γH2AX foci showed colocalization, and 73% of the foci in these cells were colocalized. However, RPA foci were detected before the appearance of the γH2AX foci. Cells that showed pan-nuclear staining of γH2AX also showed similar staining patterns for RPA.

We also determined the frequency of cells staining for γH2AX foci formation and TUNEL+ (Figure 3C). Although 53.4% of the Chk1-depleted cells showed γH2AX foci after a 48-h thymidine treatment and 12.6% were TUNEL+, only 3.6% stained for both. Thus the dramatic increase in H2AX phosphorylation in Chk1-depleted cells preceded the onset of apoptosis, but our results suggest that enhanced γH2AX is not an indicator of cellular commitment to apoptosis.

H2AX phosphorylation and foci formation occur transiently in cells exposed to IR, and this has previously been shown to reflect the time required to repair DSBs induced by this agent (Rogakou *et al.,* 1999). In control or Chk1 siRNA-treated HCT116 cells, γH2AX foci formed at 15–90 min after IR exposure (Supplemental Figure S2, B and C). Interestingly these radiation-induced γH2AX foci do not colocalize with RPA. Thus the kinetics of γH2AX induction and localization are distinctively different for Chk1-depleted cells exposed to IR relative to those exposed to replication inhibitors.

Cdc45 Depletion Suppresses H2AX Phosphorylation and the Formation of γH2AX Foci in Chk1-depleted Cells Treated with Replication Inhibitors

We previously reported that RPA foci and apoptosis induced in Chk1-depleted cells treated with replication inhibitors could be suppressed by depletion of Cdc45 (Rodriguez *et al.,* 2008). To determine whether the induction of γH2AX was also suppressed under these conditions, HCT116 cells were codepleted of Chk1 and Cdc45 and treated with thymidine for 24 or 48 h. Cells were then harvested and analyzed for γH2AX and RPA34 by Western blotting, or cells were fixed and stained for γH2AX foci formation. We pre-

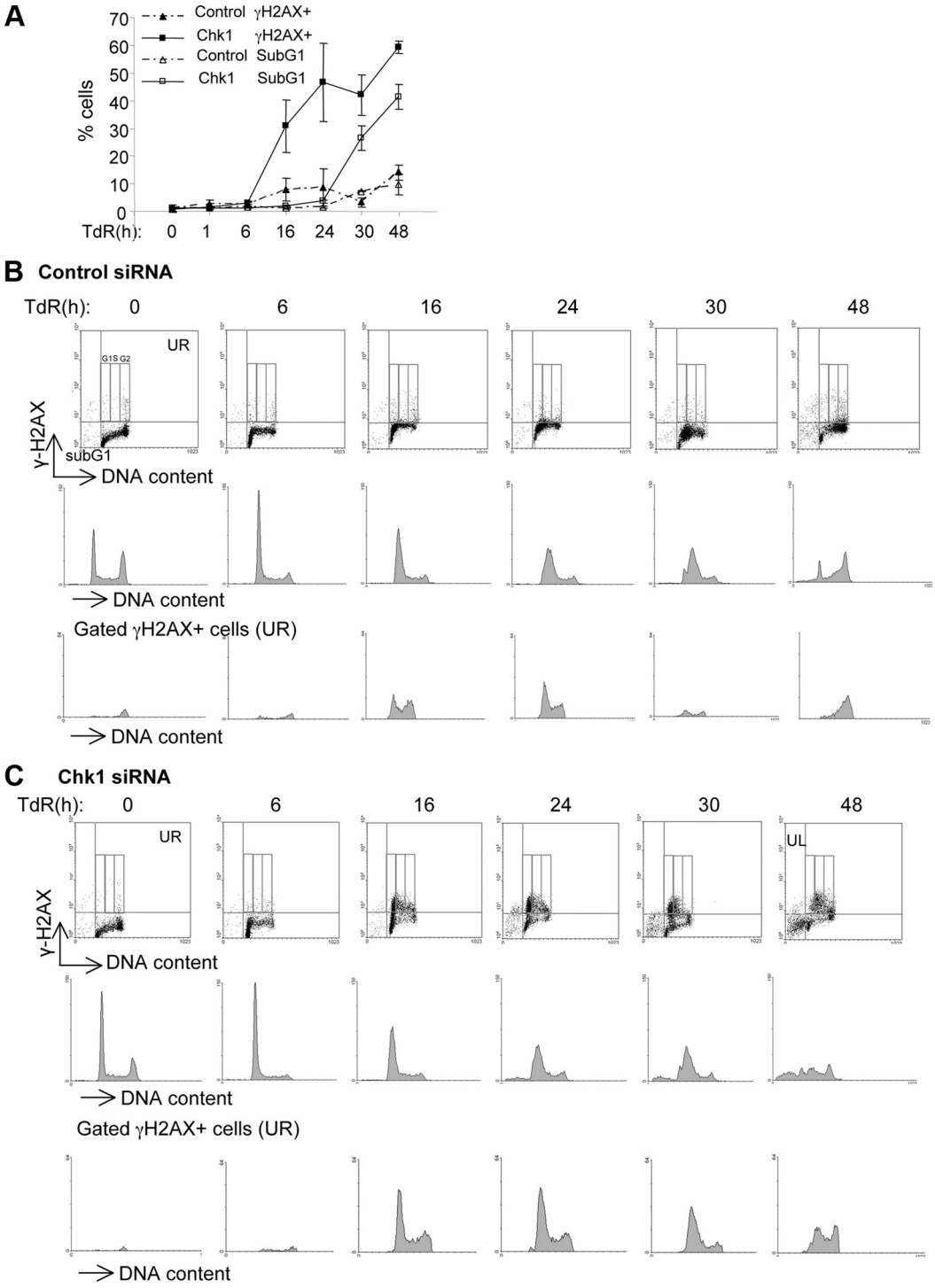

Figure 2. Kinetics of γH2AX induction after thymidine treatment of HCT116 cells transfected with control or Chk1 siRNAs. (A) Percentages (%) of γH2AX positive cells or cells with subG1 DNA contents at indicated times of 2 mM thymidine (TdR)-treatment of siRNA-transfected HCT116 cells, as measured by flow cytometry. Results in A represent the means of three independent experiments ± SDs. (B and C) Scatter plots presenting flow cytometric analysis of γH2AX fluorescence intensity and PI staining in control (B) or Chk1 (C) siRNA-transfected cells exposed to thymidine for the indicated times. Cell cycle profiles are also presented, below the corresponding γH2AX assay, for either total cells (middle panels) or cells gated for increased γH2AX staining (upper right or UR) region in the plots, lower panels). Cells with a subG1 DNA content are boxed on the left of each panel with the γH2AX-positive cells having a subG1 DNA content on the upper left (UL).

viously showed that siRNA-mediated depletion of Cdc45 slightly slowed progression through S-phase but did not significantly affect cell viability in colony forming assays or induce apoptosis. Similarly Cdc45 depletion did not stimulate H2AX phosphorylation or RPA34 hyperphosphorylation in control or thymidine-treated cells (Figure 4A). However the robust induction of γH2AX and hyperphosphorylation of RPA seen in the Chk1-depleted cells in the presence of thymidine

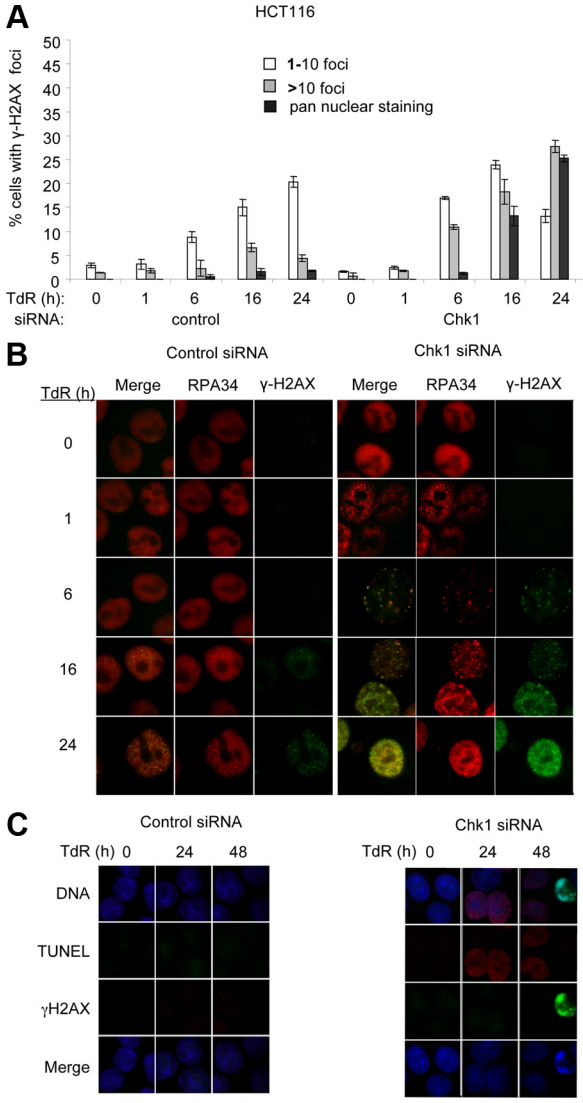

Figure 3. Nuclear distribution of γH2AX and RPA34 in HCT116 cells transfected with control or Chk1 siRNAs after thymidine treatment. (A) Percentages of HCT116 cells treated with the indicated siRNAs presenting low (1–10 foci/cell) or high (>10 foci/cell) levels of γH2AX foci or showing pan-nuclear staining after exposure to 2 mM thymidine (TdR) for the indicated times. Results represent the means of three independent experiments ± SDs. (B) Representative immunofluorescence images reveal colocalization of γH2AX and RPA foci. Colocalization of γH2AX (green) and RPA34 (red) appears as yellow in merged images. (C) HCT116 cells transfected with control or Chk1 siRNAs and exposed to 2 mM thymidine for the indicated times were stained for γH2AX or TUNEL. Most of the Chk1-depleted cells with strong γH2AX staining after 48-h exposure to thymidine were negative for TUNEL staining. TUNEL staining was only observed in cells with clear signs of apoptotic nuclear morphology. Cells were also DAPI stained for DNA (blue).

were reduced to control levels in codepleted cells (Figure 4A). Similar effects on γH2AX formation and RPA hyperphosphorylation were seen in Chk1-depleted HCT116 cells treated with a second Cdc45 siRNA and in cells treated with the Chk1 inhibitor Gö6976 instead of the siRNA (Supplemental Figure S5, A and B). Cdc45 depletion also suppressed γH2AX induction and RPA hyperphosphorylation in SW480 cells depleted of Chk1 (Supplemental Figure S5C).

To confirm this, we next examined the nuclear distribution of γH2AX in HCT116 cells transfected with control or Chk1 siRNAs after a 24-h treatment with thymidine (Figure 4, B and C). During unperturbed DNA replication, depletion of Cdc45 produced a low level of cells staining weakly (1–10 foci) for γH2AX fluorescence relative to control or Chk1-depleted cells that may reflect the slower progression through S-phase seen in such cells. This increase was not as pronounced in cells codepleted of Cdc45 and Chk1. After a 2-h exposure to thymidine, the percentages of Cdc45-depleted cells with γH2AX foci (weakly staining with 1–10 foci or showing more intense staining with >10 foci) were slightly higher than thymidine-treated control cells. Cells with pan-nuclear staining were not detected. Chk1 ablation dramatically increased the fraction of cells with >10 foci and those showing pan-nuclear staining after thymidine treatment. Codepletion of Chk1 and Cdc45 reduced the formation of γH2AX nuclear foci in arrested cells but more dramatically reduced the fraction of cells with pan-nuclear staining relative to cells treated with Chk1 siRNA. The proportion of cells staining weakly for γH2AX (<10 foci) increased in the codepleted cells relative to cells depleted of Chk1 alone but remained at the level of the control.

We also used flow cytometry to measure γH2AX and DNA content in cells depleted of Chk1 and/or Cdc45. These analyses showed that the γH2AX-positive cells that were lost after codepletion of Chk1 and Cdc45 and thymidine treatment were mainly in S-phase (Supplemental Figure S6). Collectively, the above data from immunofluorescence and FACS analyses verified the suppressive effect of Cdc45 depletion on the enhanced induction of γH2AX during replication stress in the absence of Chk1. Moreover, they indicate that the pan-nuclear distribution of γH2AX occurring in Chk1-depleted cells is particularly dependent on Cdc45 function during S-phase.

In contrast HCT116 cells deficient in p21, a negative regulator of replication origin firing, showed a more robust γH2AX induction after treatment with the Chk1 siRNA or the Chk1 inhibitor Gö6976 and exposure to thymidine relative to p21+/+ cells (Figure 4D).

Chk1-depleted Cells Fail to Recover from Thymidine-induced Arrest

To further investigate the role of γH2AX in the Chk1 suppressed pathway, we measured γH2AX levels and foci in control and Chk1-depleted cells released from thymidine treatment. We first determined the reversibility of thymidine treatment in control and Chk1-depleted HCT116 cells. DNA content in such cells was measured by FACS after continuous exposure to thymidine for 24, 32, 40, 48 or 64 h and in cultures exposed to thymidine for 24 h and then released into thymidine-free medium for 8, 16, 24 or 40 h. Control cells continuously exposed to thymidine slowly traversed S-phase and accumulated in G2 after 64-h exposure (Supplemental Figure S7). When these cells were released from thymidine after 24 h, they reentered the cell cycle and after 16 h showed a profile similar to that of untreated cells. Chk1-depleted cells showed a similar slow transition through S-phase in the presence of thymidine; however, by 40 h 27% of cells showed a subG1 DNA content, and fewer cells remained in S and G2. In Chk1-depleted cultures released into thymidine-free medium after 24 h, many cells failed to reenter the cell cycle and remained in S-phase, and 16 h after release 24% showed a subG1 DNA content, much like the cultures continuously exposed to thymidine. Measurements of activated caspase-3 together with DNA content verified the apoptotic response of Chk1-depleted cells dur-

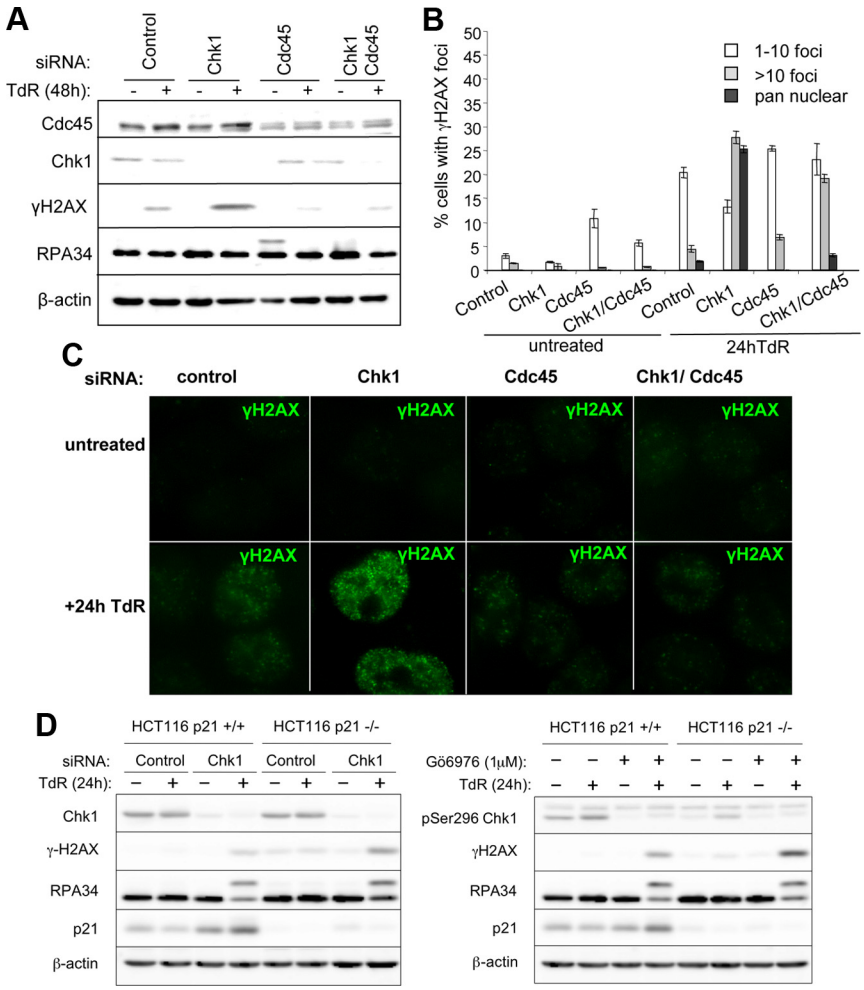

Figure 4. Cdc45 and p21 are effectors of the enhanced induction of H2AX phosphorylation or the formation of γH2AX foci during DNA replication stress in the absence of Chk1. (A) Western blot analysis of γH2AX and RPA34 in extracts obtained from HCT116 cells transfected with the indicated siRNAs and treated or not treated with 2 mM thymidine for 48 h. The levels of Chk1 and Cdc45 proteins in the cells also are presented, whereas β-actin levels are presented as loading controls. (B) Percentages of HCT116 cells treated with the indicated siRNAs presenting low (1–10 foci/cell) or high (>10 foci/cell) levels of γH2AX foci or pan-nuclear staining after exposure to 2 mM thymidine for 24 h. Results represent the means of three independent experiments ± SDs. (C) Representative images of γH2AX immunostaining of HCT116 cells treated with the indicated siRNAs after a 24-h thymidine arrest. (D) Western blot analysis of γH2AX and RPA34 in extracts prepared from p21+/+ or p21−/− HCT116 cells treated with control or Chk1 siRNAs or the Chk1 inhibitor Gö6976 and exposed or not exposed to 2 mM thymidine for 24 h. The band showing slower mobility on panel probed with the RPA34 antibody represents hyperphosphorylated forms of the protein. The levels of Chk1 in the cells treated with the indicated siRNAs are presented. Phosphorylation of Chk1 at the Ser296 autophosphorylation site was measured (lower band) to determine the effectiveness of Gö6976 treatment. β-actin levels are presented as loading control.

ing recovery from a 24-h thymidine arrest (Supplemental Figure S8). After Chk1 ablation, activation of caspase-3 was detected in S-phase during and after replication stress (31 and 24% of total cells, respectively). In contrast, both control and Chk1 siRNA-treated cells were able to reenter the cell cycle after release from a shorter (6 h) treatment with thymidine (Supplemental Figure S9A) although after a 16-h thymidine treatment the Chk1-depleted cells were largely committed to apoptosis (Supplemental Figure S9B).

We then analyzed the ability of Chk1-depleted cells to resume DNA synthesis after release from thymidine (Figure 5A). Chk1 depletion had little effect on BrdU incorporation in the absence of replication stress, with 44% of cells treated with the control siRNA and 39% of cells depleted of Chk1 incorporating BrdU in a 1-h pulse (Figure 5, B–D). To determine the effect of replication stress in such cells, control or Chk1 siRNA-treated HCT116 cells were exposed to thymidine for 24 h, before being shifted to thymidine-free medium and pulsed with BrdU for 1 h and then left to cycle for 2, 4, 6, or 20 h in thymidine- and BrdU-free medium before harvest for FACS analysis of DNA content and BrdU incorporation. In HCT116 cultures exposed to thymidine for 24 h before release, BrdU incorporation was detected in 86% of cells treated with the control siRNA and in 72% of Chk1-depleted cells. In control cultures the BrdU-positive cells progressed through S-phase and after 6 h, 69% of them were in G2. In the absence of Chk1, S-phase progression was delayed in BrdU-labeled cells. By 6 h, only 33% progressed to G2 phase. In cultures left to grow for 20 h after BrdU labeling, control cells showed a more normal cell cycle distribution, with 45% of the BrdU-labeled cells traversing the cell cycle to G1. In contrast a smaller proportion of BrdU-labeled Chk1-depleted cells appeared in G1 (22%), whereas most remained in S and G2. In addition nearly 20% of cells from these cultures had a subG1 DNA content. Thus Chk1-depleted cells show a strongly reduced capacity to reenter and traverse S-phase and a greater commitment to death after a 24-h exposure to thymidine, relative to control cells. A high proportion of Chk1-depleted cells incorporate BrdU after release but, given the reduced transition through S-phase, this may not represent the resumption of synthesis at stalled forks in some of these cells.

SW480 cells show a similar ability to rapidly reenter S-phase after thymidine or HU treatment (Supplemental Figure S10, A and B). On release from thymidine a high proportion incorporate BrdU in a 1-h pulse. By 4 h most of these cells traversed S-phase and entered G2, and by 24 h a cell cycle profile typical for growing cells is restored. For Chk1-depleted SW480 cells, a much smaller proportion reenter S-phase. Strikingly, a large number of cells with an S-phase DNA content fail to incorporate BrdU in the 1-h pulse. By 4 h after release there is very little change in the cell cycle profile, and only a small proportion of the cells incorporating BrdU appear to have progressed to G2, and by 24 h after release there is still little change in the cell cycle profile suggesting that only a fraction of the cells incorporating

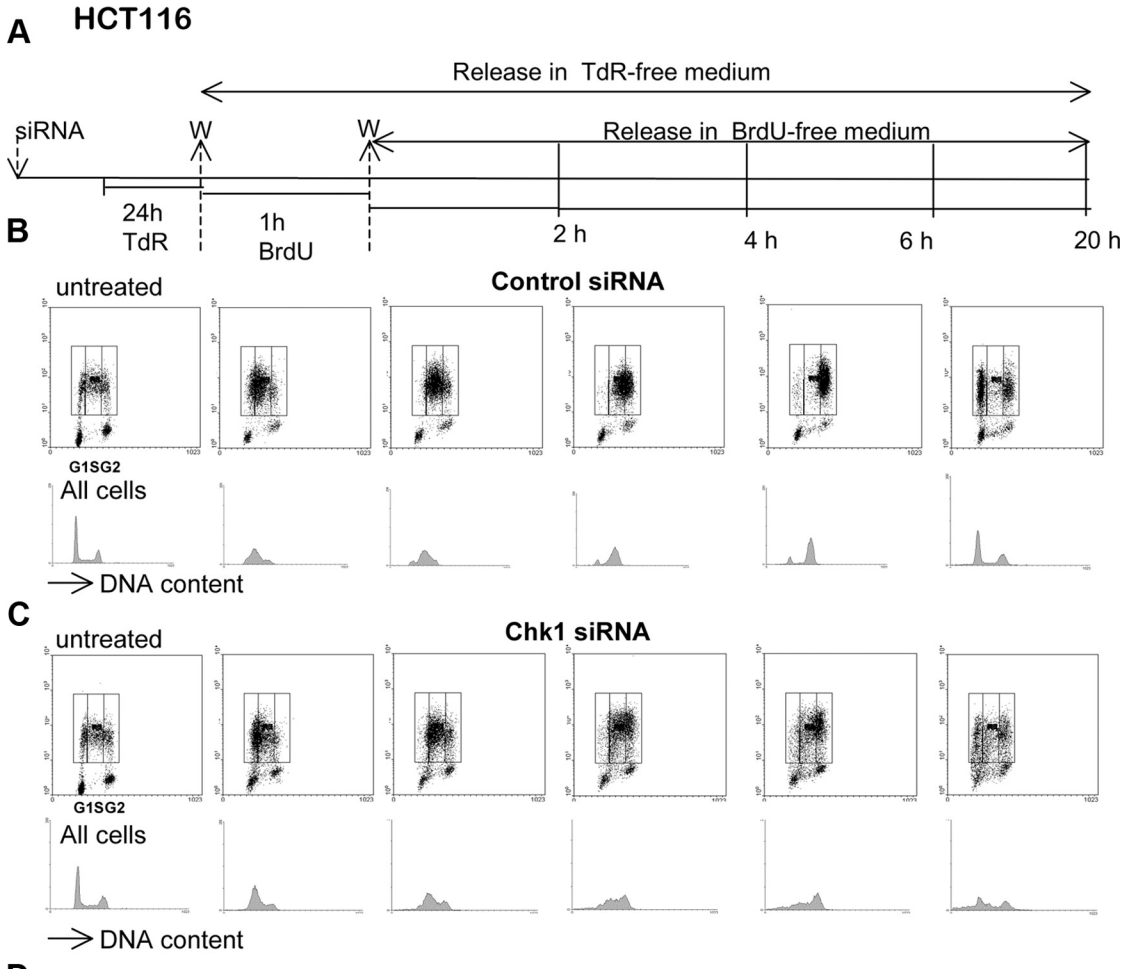

D

	%BrdU incorporation					
Hours * :	**-****	**0**	**2**	**4**	**6**	**20**
Control siRNA :						
G1/S	12.00 ± 1.60	14.17 ± 6.63	4.00 ± 0.20	1.26 ± 0.06	3.09 ± 0.09	45.18 ± 1.58
S	19.48 ± 2.78	63.10 ± 5.80	68.70 ± 1.40	47.67 ± 1.77	15.40 ± 0.50	10.25 ± 0.35
G2	12.43 ± 2.23	8.49 ± 2.19	14.35 ± 0.55	37.65 ± 1.45	68.71 ± 2.01	27.90 ± 1.50
Total	43.86 ± 6.66	85.77 ± 1.37	87.05 ± 2.15	86.53 ± 3.33	87.20 ± 2.60	83.34 ± 3.44
Chk1 siRNA :						
G1/S	9.74 ± 1.45	29.35 ± 2.45	9.05 ± 1.15	4.73 ± 1.66	7.10 ± 0.90	22.40 ± 2.70
S	16.74 ± 0.24	37.25 ± 3.15	52.46 ± 3.74	42.05 ± 5.15	32.87 ± 3.52	18.38 ± 3.31
G2	12.86 ± 1.86	4.95 ± 0.15	13.17 ± 0.62	26.45 ± 0.34	33.17 ± 0.97	25.77 ± 0.77
Total	39.30 ± 0.70	71.55 ± 5.44	74.68 ± 5.51	73.19 ± 7.11	73.09 ± 3.40	66.61 ± 5.29

* after release in BrdU - and TdR - free medium

** normal cycling cells (no TdR treatment)

Figure 5. Chk1-depleted HCT116 cells released from thymidine treatment remain committed to apoptosis and show suppressed reentry into S-phase. (A) HCT116 cells transfected with control or Chk1 siRNAs and exposed to 2 mM thymidine for 24 h were washed (W) with thymidine-free medium and transferred to medium containing 10 μM BrdU. After 1 h these cells were washed with BrdU-free medium and harvested for FACS analysis at the indicated times. (B and C) Representative scatter plots (top panels) show BrdU incorporation and DNA content (PI staining) in cells transfected with control (B) or Chk1 siRNAs (C) as described above. Cells incorporating BrdU have been gated (as indicated) to determine the percentages with G1, S, or G2 DNA content. Cells with a G1 DNA content incorporating BrdU at early times after the pulse most likely represent cells at the G1/S border, although at 20 h these are likely to represent cells that have traversed the cell cycle and reentered G1. Bottom panels present DNA content (PI staining) of all the cells in the cultures (gated and ungated). Cells indicated as untreated present BrdU incorporation of cells before thymidine treatment. (D) Table summarizing the cell cycle distributions and total cells incorporating BrdU treated as described in B and C. Results represent the means of three independent experiments ± SDs.

BrdU have resumed growth. SW480 cells released from HU show a slower reentry into S-phase. At 4 h the cells largely remain in S-phase and 40% are in G2 at 24 h. In Chk1-depleted SW480 cells only 15–16% incorporate BrdU after the 24-h exposure to HU and the cell cycle profile is largely unchanged over 24 h. Thus like HCT116 cells, Chk1-depleted SW480 cells show a strongly reduced ability to reenter and traverse S-phase after release from treatment with replication inhibitors.

γH2AX Foci Persist in Chk1-depleted Cells Released from Replication Stress

We next examined γH2AX status in cells released from thymidine treatment. HCT116 cells transfected with control or Chk1 siRNAs and exposed to thymidine for 24 h were released into thymidine-free medium or left to grow in the inhibitor for another 24 h before harvest. Western blot analysis of total protein extracts from the above cultures showed a decrease in the level of γH2AX in Chk1-depleted cells released from thymidine although it remained considerably higher than in control cells treated with thymidine. Hyperphosphorylated RPA34 showed a gradual decline and was barely detectable at 24 h after release (Figure 6A). This is accompanied by a sustained activation of ATM (in the form of pSer1981 ATM) and Chk2 (pThr68 Chk2) in the thymidine-released cells. A similar pattern of sustained activation of H2AX, ATM, and Chk2 were also found in Chk1-depleted HCT116 cells treated with HU for 24 h and then released (data not presented) and in SW480 cells treated with thymidine or HU for 24 h and then released (Supplemental Figure S11A).

In addition we measured γH2AX foci in Chk1-depleted cells recovering from thymidine arrest (Figure 6, B and C). After release from a 24-h thymidine treatment the fraction of cells showing >10 γH2AX foci decreased slightly, whereas there was a larger fall in the fraction of cells showing pannuclear γH2AX staining. We further measured the levels of γH2AX accumulation in Chk1-depleted HCT116 cells together with DNA content by flow cytometry as described above (Figure 6D). This analysis revealed that the fraction of cells positive for γH2AX showed a progressive decline at 24 and 40 h after release relative to the fraction measured before release (Figure 6, D and E), whereas only a small proportion of control cells showed γH2AX under the same conditions. Interestingly only a very small proportion of cells staining for increased γH2AX (0.39–0.55%) had a subG1 DNA content at 24 or 40 h after release even though the percentage of total cells in these cultures with a subG1 DNA content was significantly higher at these times relative to the Chk1-depleted cells treated with thymidine for 24 h (Figure 6, D and E). Chk1-depleted SW480 cells produced similar results with respect to γH2AX foci after thymidine treatment (Supplemental Figure S11, B and C) and FACS-based analysis of γH2AX levels after thymidine or HU (Supplemental Figure S11D). Taken together these data indicate that γH2AX persists in a high proportion of Chk1-depleted cells released from thymidine, although our data indicate that some dephosphorylation of γH2AX and loss of foci occurs in these cells. Furthermore, cells containing elevated levels of γH2AX have a low level of apoptosis.

Most of the cells having increased γH2AX after exposure to thymidine for 24 h had a G1/S-phase DNA content, whereas the cells released from thymidine for 24 h showed a broader distribution (Figure 6D). This is similar to our previous observation that Chk1-depleted cells labeled with BrdU showed a prolonged transition through S-phase after release (Figure 5C). In view of the slow transition of γH2AX-positive cells through S-phase during recovery from thymidine arrest in the absence of Chk1 despite the incorporation of BrdU in a high proportion of cells in these cultures, we next examined BrdU incorporation in cells containing γH2AX foci by immunofluorescence. In Chk1-depleted cultures treated with thymidine for 16 h and then released into thymidine-free medium containing BrdU, only 16% of total cells stained for both γH2AX and BrdU incorporation (Figure 7, A and B). Strikingly, BrdU incorporation was detected in only 35% of all cells showing γH2AX foci and not at sites of these foci (Figure 7A and B). Additionally, 54% of cells showed BrdU incorporation but no γH2AX foci and 30% showed only γH2AX foci.

Very similar responses were found with Chk1-depleted SW480 cells (Figure 7C). Only ~19% of Chk1-depleted cells showed both γH2AX foci and BrdU incorporation and, as with HCT116 cells, BrdU incorporation was not detected at sites of γH2AX foci. As found previously a lower percentage of Chk1-depleted SW480 cells incorporated BrdU after release from thymidine.

Similarly RPA foci found in Chk1-depleted HCT116 cells after 16-h thymidine treatment and release into medium containing BrdU do not colocalize with sites of BrdU incorporation (Figure 7D). However consistent with earlier results, the RPA foci detected in these experiments show a high level of colocalization with γH2AX foci (Figure 7E).

Cells Showing Persistent γH2AX Are Less Likely to Undergo Apoptosis

FACS analysis of γH2AX levels and DNA content revealed that cells with a subG1 DNA content did not contain enhanced levels of γH2AX (Figure 6D). To further examine the relationship between γH2AX and the induction of death by replication inhibitors in Chk1-depleted cells, we measured caspase-3 activation in cells showing γH2AX induction. HCT116 cells treated with control or Chk1 siRNAs were exposed to thymidine for 24 or 48 h or treated with thymidine for 24 h and released into thymidine-free medium for 24 h before being fixed and stained for activated caspase-3, γH2AX, and DNA content by immunofluorescence analysis as described above. Chk1-depleted cells showing activated caspase-3 did not stain for γH2AX, whereas those staining for γH2AX did not show activated caspase-3 (Figure 8A).

Taken together our data suggest that γH2AX foci persist at stalled forks in cells showing aberrant progression through S-phase in the absence of Chk1. This is accompanied by chronic activation of the ATM-mediated signaling cascade but not the induction of apoptosis.

DISCUSSION

After the disruption of DNA replication cells rapidly activate both ATM and ATR-mediated signaling cascades to protect the integrity of DNA (Zhou and Elledge, 2000; Bolderson *et al.*, 2004). Work from several labs indicates that the ATR-Chk1 pathway plays a critical role in protecting cells from apoptosis under these conditions (Cho *et al.*, 2005; Rodriguez and Meuth, 2006; Xiao *et al.*, 2005). γH2AX formation has normally been associated with the induction DSBs after exposure to IR or other DNA-damaging agents (Rogakou *et al.*, 1998). However, a number of reports have shown phosphorylation of H2AX after DNA replication stress (Ward and Chen, 2001; Furuta *et al.*, 2003; Ewald *et al.*, 2007) that is enhanced in Chk1-inhibited cells (Furuta *et al.*, 2006; Ewald *et al.*, 2007). Given the association of this enhanced γH2AX formation and cell death when Chk1 function is compromised, we further investigated the changes in

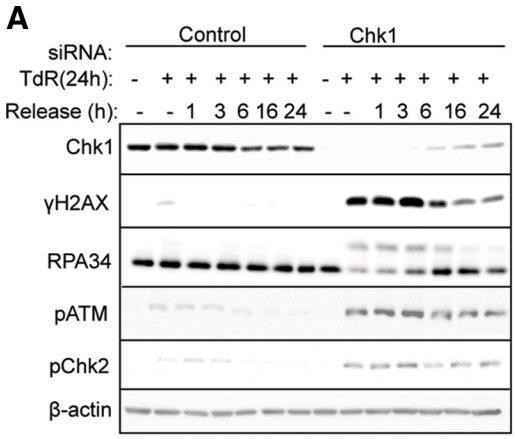

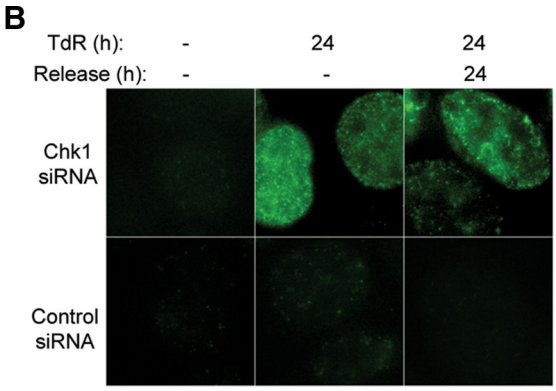

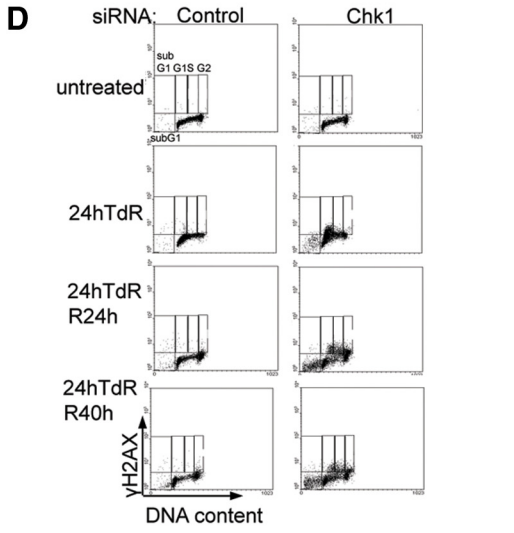

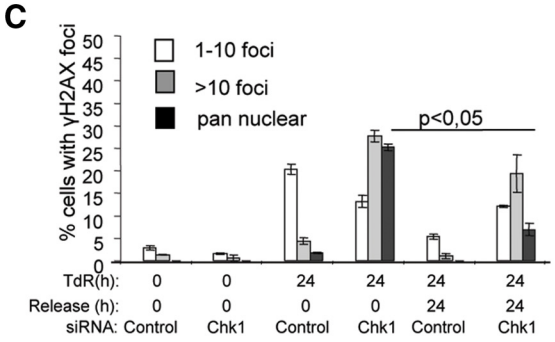

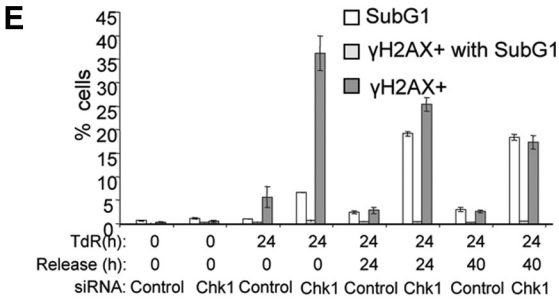

	TdR(h) :	0	24	24	24
	Rec(h) :	0	0	24	40
	Control siRNA				
	Total SubG1	0.69 ± 0.06	1.02 ± 0.01	2.44 ± 0.22	3.04 ± 0.39
%γH2AX+	SubG1	0.07 ± 0.01	0.31 ± 0.05	0.47 ± 0.05	0.31 ± 0.03
	G1/S	0.08 ± 0.01	1.30 ± 0.40	0.29 ± 0.04	0.25 ± 0.02
	S	0.03 ± 0.01	1.70 ± 0.99	0.28 ± 0.02	0.26 ± 0.01
	G2	0.21 ± 0.07	2.68 ± 0.88	2.25 ± 0.55	2.04 ± 0.24
	Chk1 siRNA				
	Total SubG1	1.14 ± 0.09	6.60 ± 0.03	19.12 ± 0.55	18.37 ± 0.61
%γH2AX+	SubG1	0.22 ± 0.02	0.66 ± 0.16	0.39 ± 0.08	0.55 ± 0.01
	G1/S	0.07 ± 0.01	26.09 ± 2.24	5.85 ± 0.30	4.36 ± 0.36
	S	0.17 ± 0.05	7.09 ± 1.19	8.30 ± 0.35	6.00 ± 0.45
	G2	0.27 ± 0.09	3.07 ± 0.27	11.26 ± 0.81	6.96 ± 0.61

Figure 6. Persistence of γH2AX and other DNA damage response proteins in Chk1-depleted cells after release from thymidine arrest. (A) Western blot analysis of γH2AX, RPA34, phospho-ATM (pSer1981), and phospho-Chk2 (pThr68) in extracts obtained from HCT116 cells transfected with control or Chk1 siRNAs and treated or not treated with 2 mM thymidine (TdR) for 24 h before release into thymidine-free medium for the indicated times. The levels of Chk1 protein in the cells also are presented, whereas β-actin levels are presented as loading controls. (B) Representative immunofluorescence images of γH2AX nuclear distribution in siRNA-transfected HCT116 cells treated with thymidine for 24 h or treated and released from thymidine for 24 h. (C) Percentages of HCT116 cells treated with control or Chk1 siRNAs presenting low (1–10 foci/cell) or high (>10 foci/cell) levels of γH2AX foci or showing pan-nuclear staining for γH2AX during and after exposure to thymidine for the indicated times. Results presented are the means of three independent experiments ± SDs. (D) Representative scatter plots illustrating flow cytometric analysis of γH2AX levels and DNA content of siRNA-transfected HCT116 cells treated with 2 mM thymidine for 24 h and then released for 24 or 40 h before harvest. γH2AX+ cells with subG1, G1, S, or G2 DNA contents are gated. γH2AX+ cells having a subG1 DNA content are in the top left boxes, whereas the total cells with a subG1 DNA content are present in the top left and bottom left boxes. The table summarizes the cell cycle distributions of the γH2AX+ cells and the total cells with a subG1 DNA content. Values represent the means of three independent experiments ± SDs. (E) Percentages (%) of γH2AX+ cells, γH2AX+ cells with a subG1 DNA content, and total cells with a subG1 DNA content in siRNA-transfected HCT116 cultures as measured by flow cytometry in D. Results represent the means of three independent experiments ± SDs.

H2AX phosphorylation in such cells during DNA replication stress. Here we show that H2AX phosphorylation and foci formation occur well in advance of DNA fragmentation or caspase-3 activation after the disruption of replication in

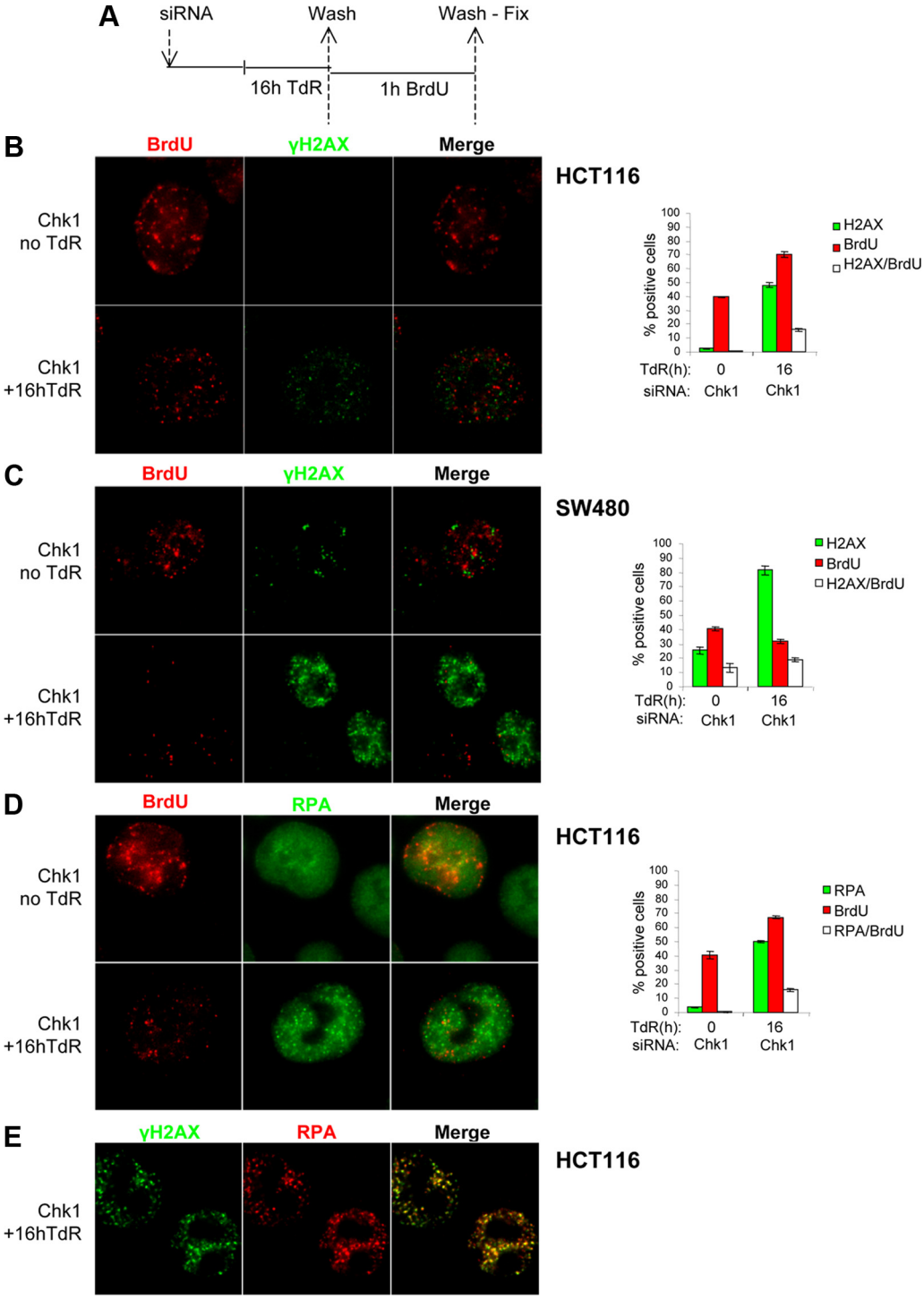

Figure 7. BrdU incorporation does not coincide with γH2AX or RPA foci after release of Chk1-depleted HCT116 cells from thymidine. (A) HCT116 or SW480 cells transfected with the Chk1 siRNA were treated or not treated with 2 mM thymidine (TdR) for 16 h before release into thymidine-free medium containing 10 μM BrdU for 1 h. Cells were fixed and stained for BrdU incorporation or γH2AX, immunofluorescence images of BrdU incorporation with γH2AX distribution in HCT116 (B), or SW480 (C) cells treated as above. The adjacent graphs show the percentages of Chk1-depleted cells showing γH2AX or BrdU staining or both. Notably, BrdU incorporation was not detected at the sites of γH2AX foci in either cell line. (D) HCT116 cells treated as in A were stained for BrdU incorporation and RPA34. BrdU incorporation was not detected at nuclear sites of RPA34 foci. (E) Representative immunofluorescence images showing colocalization of γH2AX and RPA34 foci in Chk1-depleted HCT116 cells treated with thymidine for 16 h before release as above.

the absence of Chk1 in two colon cancer cell lines. γH2AX foci largely colocalize with RPA foci that form in such cells indicating that H2AX phosphorylation occurs at the site of disrupted replication forks. The pan-nuclear staining of γH2AX occurring in a subset of Chk1-depleted cells is a distinctive feature of this response. A similar pattern of

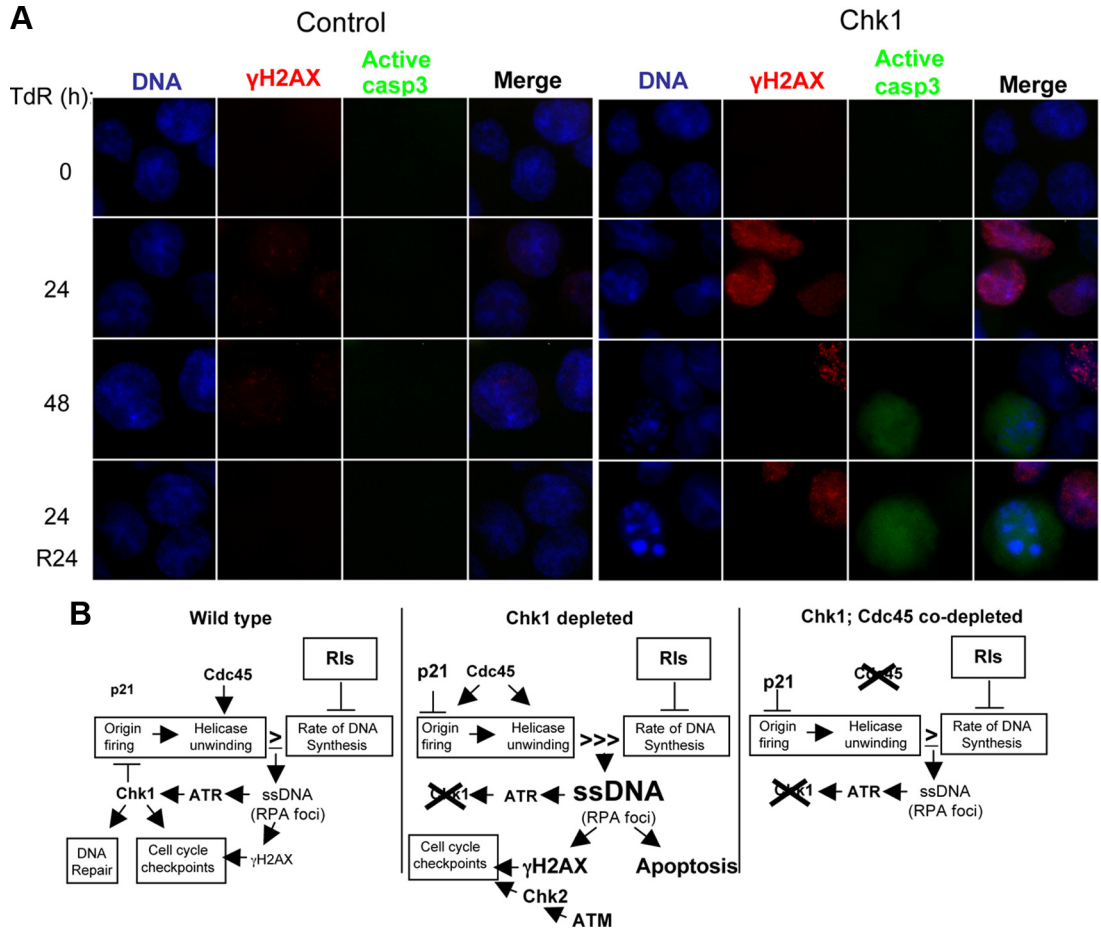

Figure 8. Cells with persistent γH2AX foci do not contain activated caspase-3. (A) HCT116 transfected with control or Chk1 siRNAs were exposed to 2 mM thymidine for the indicated times or exposed to thymidine for 24 h followed by a 24-h release into thymidine-free medium. Cells were then fixed and stained for γH2AX and active caspase-3. Cells staining for γH2AX foci did not show activated caspase-3. Similarly cells staining for caspase-3 (that also showed a nuclear structure characteristic of apoptotic cells) did not stain for γH2AX. (B) Proposed model for the role of γH2AX in the Chk1 suppressed death pathway responding to DNA replication stress. ATR-mediated Chk1 activation is crucial to maintain cell viability and genome stability upon replication stress, by regulating fork integrity, replication restart, and inappropriate origin firing in response to replication inhibitors (RIs, left). In the absence of Chk1, the action of Cdc45 on origin firing and helicase unwinding increases the level ssDNA in cells, triggering a caspase-3–dependent apoptotic pathway in S-phase cells (middle). The data presented here suggest that γH2AX formation is enhanced in Chk1-depleted cells in response to persistent stress at DNA replication forks that also leads to prolonged ATM and Chk2 activation. The accumulation of γH2AX is also dependent on Cdc45, but the signal triggering H2AX phosphorylation is not clear (right). Our results suggest that γH2AX may help protect some cells from apoptosis, perhaps through maintaining S-phase checkpoints. However, H2AX phosphorylation does not appear to be sufficient for the restart of DNA replication in the absence of Chk1 as DNA replication is not detected at sites of γH2AX foci after release from the replication inhibitor.

γH2AX staining that is independent of DNA DSB formation and dependent on nucleotide excision repair has previously been observed with primary human fibroblasts after UV irradiation (Marti *et al.*, 2006). Here we show that this widespread phosphorylation of H2AX is particularly dependent on the function of the essential replication helicase cofactor Cdc45 as there is a pronounced loss of cells showing pan-nuclear staining after Cdc45 depletion. Because Cdc45 is a component of a protein complex involved in DNA replication initiation in human cells (Bauerschmidt *et al.*, 2007; Aparicio *et al.*, 2009), these observations suggest that the widespread phosphorylation may be promoted by the inappropriate firing of late or cryptic origins dispersed through the genome upon suppression of Chk1 function (Maya-Mendoza *et al.*, 2007). Consistent with this argument, γH2AX formation is enhanced in cells deficient in p21 that negatively affects the G1→S transition and origin firing through inhibition of cyclin-dependent kinase (El-Deiry *et al.*, 1993; Xiong *et al.*, 1993). Both Cdc45 and p21 also affect replication elongation; however, the effects of these proteins on apoptosis (Rodriguez *et al.*, 2008) and γH2AX formation are only seen in cells depleted of Chk1 where inappropriate origin firing occurs (Maya-Mendoza *et al.*, 2007).

After release of Chk1-depleted cells from thymidine, γH2AX persists in a high proportion of cells. Because BrdU incorporation does not occur at persistent γH2AX foci, they are unlikely to represent sites of fork rescue despite their colocalization with RPA34. Therefore, we propose that these γH2AX foci represent sites of persistent unresolved or abandoned forks that may also trigger the ATM and Chk2 activation observed here. The nature of the lesions triggering this chronic response is not clear. They are not likely to be persistent DSBs as these are not detectable in Chk1-depleted cells by pulsed field gel electrophoresis (Rodriguez *et al.*, 2008). Given the sensitivity of these pulsed field gels (~40 breaks/cell as measured using cells exposed to low levels of

IR), we cannot eliminate the possibility that a low level of breaks may be transiently produced at some stalled forks. However, the large number of γH2AX foci and pan-nuclear staining seen in the Chk1-depleted cells treated with replication inhibitors indicate that such DSBs would not be widespread at such sites. We speculate that the BrdU incorporation occurring at sites distinct from γH2AX foci in such cells may represent cryptic origins that were activated in the absence of Chk1 and incorporate BrdU once the cells were released from the replication inhibitor, although they may also represent origins that have successfully restarted replication after dephosphorylation of γH2AX.

Despite the persistence of γH2AX foci in some cells, they do not appear to be committed to apoptosis. Cells strongly staining for γH2AX do not have a subG1 DNA content, are not TUNEL+, and do not show activated caspase-3. When Chk1-depleted cells are released from the replication inhibitor, a subset of cells remain committed to apoptosis. Those showing persistent γH2AX slowly traverse S-phase but do not die. The persistent activation of ATM and its downstream target Chk2 seen under these conditions is likely to contribute to the retarded progression through S-phase. The kinetics of γH2AX formation in response to replication stress reported here adds to the complexity of its regulation and suggests that γH2AX may interfere with the ability of cells to become committed to apoptosis in the absence of Chk1. Reports that γH2AX may be phosphorylated by multiple kinases such as ATM, ATR, DNA-PK, or JNK (Ward and Chen, 2001; Stiff *et al.*, 2005; Lu *et al.*, 2006) indicate that γH2AX can act as a transducer of multiple upstream events. Therefore, γH2AX may help integrate and coordinate many of the early events after replication fork stalling with later events such as repair (Paull *et al.*, 2000; Xie *et al.*, 2004) and replication restart depending on the appropriate firing of replication origins. However in the absence of Chk1 the repair/restart function may be compromised (Figure 8B). Chk1 then occupies a central role in the regulation of cell death in response to replication inhibitors through its multiple roles in controlling replication restart and origin firing during stress.

It is important to note that one of the cell lines used in these experiments (HCT116) has been shown to carry a mutation of Mre11 (Giannini *et al.*, 2002) that compromises the activation of Chk2 (Takemura *et al.*, 2006) and ATM (Wen *et al.*, 2008) after some types of DNA replication stress. However the second colon cancer cell line used in these experiments (SW480) does not have a mutation of Mre11 and shows a more normal activation of the ATM signaling cascade after replication stress. The similar responses obtained here with the two different colon cancer cell lines is consistent with previous work from our laboratory showing that ATM, Chk2, Mre11, and NBS1 are not determinants of the induction of cell death by replication inhibitors (Rodriguez and Meuth, 2006; Myers *et al.*, 2009). It is intriguing that Chk1 depletion restores ATM and Chk2 activation in HCT116 cells during DNA replication stress. We have previously proposed that cells defective in Mre11 function may be compromised in their ability to process stressed DNA replication forks into forms that activate this signaling pathway. We speculate that in the absence of Chk1 alternative intermediates (perhaps in the form of abandoned forks) may be produced at stalled forks that activate this signaling cascade.

There is increasing interest in the use of γH2AX as a biomarker for DNA damage in response to environmental stress or the efficacy of therapeutic agents in cancer patients (Bonner *et al.*, 2008). The work reported here indicates that γH2AX can be an effective indicator of irreversible DNA replication fork arrest but not apoptosis.

ACKNOWLEDGMENTS

We are grateful to Helen Bryant for critically reading the manuscript. This work was supported by a program grant from Yorkshire Cancer Research to M.M.

REFERENCES

Aparicio, T., Guillou, E., Coloma, J., Montoya, G., and Mendez, J. (2009). The human GINS complex associates with Cdc45 and MCM and is essential for DNA replication. Nucleic Acids Res. *37*, 2087–2095.

Ball, H. L., Myers, J. S., and Cortez, D. (2005). ATRIP binding to Replication Protein A-single-stranded DNA promotes ATR-ATRIP localization but is dispensable for Chk1 phosphorylation. Mol. Biol. Cell *16*, 2372–2381.

Bauerschmidt, C., Pollok, S., Kremmer, E., Nasheuer, H.-P., and Grosse, F. (2007). Interactions of human Cdc45 with the Mcm2–7 complex, the GINS complex, and DNA polymerases δ and ε during S phase. Genes Cell. *12*, 745–758.

Beckerman, R., Donner, A. J., Mattia, M., Peart, M. J., Manley, J. L., Espinosa, J. M., and Prives, C. (2009). A role for Chk1 in blocking transcriptional elongation of p21 during the S-phase checkpoint. Genes Dev. *23*, 1364–1377.

Bolderson, E., Scorah, J., Helleday, T., Smythe, C., and Meuth, M. (2004). ATM is required for the cellular response to thymidine induced replication fork stress. Hum. Mol. Genet. *13*, 2937–2945.

Bonner, W. M., Redon, C. E., Dickey, J. S., Nakamura, A. J., Sedelnikova, O. A., Solier, S., and Pommier, Y. (2008). γH2AX and cancer. Nat. Rev. Cancer *8*, 957–967.

Byun, T. S., Pacek, M., Yee, M. C., Walter, J. C., and Cimprich, K. A. (2005). Functional uncoupling of MCM helicase and DNA polymerase activities activates the ATR-dependent checkpoint. Genes Dev. *19*, 1040–1052.

Celeste, A., *et al.* (2002). Genetic instability in mice lacking histone H2AX. Science *296*, 922–927.

Cho, S. H., Toouli, C. D., Fujii, G. H., Crain, C., and Parry, D. (2005). Chk1 is essential for tumor cell viability following activation of the replication checkpoint. Cell Cycle *4*, 131–139.

Cimprich, K. A., and Cortez, D. (2008). ATR: an essential regulator of genome integrity. Nat. Rev. Mol. Cell Biol. *9*, 616–627.

Cowell, I. G., Sunter, N. J., Singh, P. B., Austin, C. A., Durkacz, B. W., and Tilby, M. J. (2007). gH2AX foci form preferentially in euchromatin after ionising radiation. PLoS One 2e1057.

El-Deiry, W. S., Tokino, T., Velculescu, V. E., Levy, D. B., Parsons, R., Trent, J. M., Lin, D., Mercer, W. E., Kinzler, K. W., and Vogelstein, B. (1993). WAF1, a potential mediator of p53 tumor suppression. Cell *75*, 817–825.

Ewald, B., Sampath, D., and Plunkett, W. (2007). H2AX phosphorylation marks gemcitabine-induced stalled replication forks and their collapse upon checkpoint abrogation. Mol. Cancer Ther. *6*, 1239–1248.

Feijoo, C., Hall-Jackson, C., Wu, R., Jenkins, D., Leitch, J., Gilbert, D. M., and Smythe, C. (2001). Activation of mammalian Chk1 during DNA replication arrest: a role for Chk1 in the intra-S phase checkpoint monitoring replication origin firing. J. Cell Biol. *154*, 913–923.

Furuta, T., Hayward, R. L., Meng, L. H., Takemura, H., Aune, G. J., Bonner, W. M., Aladjem, M. I., Kohn, K. W., and Pommier, Y. (2006). p21CDKN1A allows the repair of replication-mediated DNA double-strand breaks induced by topoisomerase I and is inactivated by the checkpoint kinase inhibitor 7-hydroxystaurosporine. Oncogene *25*, 2839–2849.

Furuta, T., *et al.* (2003). Phosphorylation of histone H2AX and activation of Mre11, Rad50, and Nbs1 in response to replication-dependent DNA double-strand breaks induced by mammalian DNA topoisomerase I cleavage complexes. J. Biol. Chem. *278*, 20303–20312.

Giannini, G., Ristori, E., Cerignoli, F., Rinaldi, C., Zani, M., Viel, A., Ottini, L., Crescenzi, M., Martinotti, S., Bignami, M., Frati, L., Screpanti, I., and Gulino, A. (2002). Human MRE11 is inactivated in mismatch repair-deficient cancers. EMBO Rep. *3*, 248–254.

Kohn, E. A., Yoo, C. J., and Eastman, A. (2003). The protein kinase C inhibitor Go6976 is a potent inhibitor of DNA damage-induced S and G2 cell cycle checkpoints. Cancer Res. *63*, 31–35.

Lu, C., Zhu, F., Cho, Y.-Y., Tang, F., Zykove, T., Ma, W.-y., Bode, A. M., and Dong, Z. (2006). Cell apoptosis: requirement of H2AX in DNA ladder formation, but not for the activation of caspase-3. Mol. Cell *23*, 121–132.

Marti, T. M., Hefner, E., Feeney, L., Natale, V., and Cleaver, J. E. (2006). H2AX phosphorylation within the G1 phase after UV irradiation depends upon nucleotide excision repair and not double-strand breaks. Proc. Natl. Acad. Sci USA *103*, 9891–9896.

Maya-Mendoza, A., Petermann, E., Gillespie, D. A., Caldecott, K. W., and Jackson, D. A. (2007). Chk1 regulates the density of active replication origins during the vertebrate S phase. EMBO J. *26*, 2719–2731.

Myers, K., Gagou, M. E., Zuazua-Villar, P., Rodriguez, R., and Meuth, M. (2009). ATR and Chk1 suppress a caspase-3-dependent apoptotic response following DNA replication stress. PLoS Genet. *5*, e1000324.

Nghiem, P., Park, P. K., Kim, Y., Vaziri, C., and Schreiber, S. L. (2001). ATR inhibition selectively sensitizes G1 checkpoint-deficient cells to lethal premature chromatin condensation. Proc. Natl. Acad. Sci. USA *98*, 9092–9097.

Paull, T. T., Rogakou, E. P., Yamazaki, V., Kirchgessner, C. U., Gellert, M., and Bonner, W. M. (2000). A critical role for histone H2AX in recruitment of repair factors to nuclear foci after DNA damage. Curr. Biol. *10*, 886–895.

Rodriguez, R., Gagou, M. E., and Meuth, M. (2008). Apoptosis induced by replication inhibitors in Chk1-depleted cells is dependent upon the helicase cofactor Cdc45. Cell Death Differ. *15*, 889–898.

Rodriguez, R., and Meuth, M. (2006). Chk1 and p21 cooperate to prevent apoptosis during DNA replication fork stress. Mol. Biol. Cell *17*, 402–412.

Rogakou, E. P., Boon, C., Redon, C., and Bonner, W. M. (1999). Megabase chromatin domains involved in DNA double-strand breaks in vivo. J. Cell Biol. *146*, 905–916.

Rogakou, E. P., Nieves-Neira, W., Boon, C., Pommier, Y., and Bonner, W. M. (2000). Initiation of DNA fragmentation during apoptosis induces phosphorylation of H2AX histone at serine 139. J. Biol. Chem. *275*, 9390–9395.

Rogakou, E. P., Pilch, D. R., Orr, A. H., Ivanova, V. S., and Bonner, W. M. (1998). DNA double-stranded breaks induce histone H2AX phosphorylation on serine 139. J. Biol. Chem. *273*, 5858–5868.

Sengupta, S., *et al.* (2004). Functional Interaction between BLM helicase and 53BP1 in a Chk1-mediated pathway during S-phase arrest. J. Cell Biol. *166*, 801–813.

Sidi, S., *et al.* (2008). Chk1 suppresses a caspase-2 apoptotic response to DNA damage that bypasses p53, Bcl-2, and caspase-3. Cell *133*, 2110–2118.

Sorensen, C. S., Hansen, L. T., Dziegielewski, J., Syljuasen, R. G., Lundin, C., Bartek, J., and Helleday, T. (2005). The cell-cycle checkpoint kinase Chk1 is required for mammalian homologous recombination repair. Nat. Cell Biol. *7*, 195–201.

Stiff, T., O'Driscoll, M., Rief, N., Iwabuchi, K., Lobrich, M., and Jeggo, P. A. (2005). ATM and DNA-PK function redundantly to phosphorylate H2AX after exposure to ionizing radiation. Cancer Res. *64*, 2390–2396.

Stucki, M., Clapperton, J. A., Mohammad, D., Yaffe, M. B., Smerdon, S. J., and Jackson, S. P. (2005). MDC1 directly binds phosphorylated histone H2AX to regulate cellular responses to DNA double-strand breaks. Cell *123*, 333–344.

Syljuasen, R. G., Sorensen, C. S., Hansen, L. T., Fugger, K., Lundin, C., Johansson, F., Helleday, T., Sehested, M., Lukas, J., and Bartek, J. (2005). Inhibition of human Chk1 causes increased initiation of DNA replication, phosphorylation of ATR targets, and DNA breakage. Mol. Cell. Biol. *25*, 3553–3562.

Takemura, H., Rao, V. A., Sordet, O., Furuta, T., Miao, Z. H., Meng, L., Zhang, H., and Pommier, Y. (2006). Defective Mre11-dependent activation of Chk2 by ataxia telangiectasia mutated in colorectal carcinoma cells in response to replication-dependent DNA double strand breaks. J. Biol. Chem. *281*, 30814–30823.

Ward, I. M., and Chen, J. (2001). Histone H2AX is phosphorylated in an ATR-dependent manner in response to replicational stress. J. Biol. Chem. *276*, 47759–47762.

Wen, Q., Scorah, J., Phear, G., Rodgers, G., Rodgers, S., and Meuth, M. (2008). A mutant allele of MRE11 found in mismatch repair deficient tumor cells suppresses the cellular response to DNA replication fork stress in a dominant negative manner. Mol. Biol. Cell *19*, 1693–1705.

Xiao, Z., Xue, J., Sowin, T. J., Rosenberg, S. H., and Zhang, H. (2005). A novel mechanism of checkpoint abrogation conferred by Chk1 downregulation. Oncogene *24*, 1403–1411.

Xie, A., Puget, N., Shim, I., Odate, S., Jarzyna, I., Bassing, C. H., Alt, F. W., and Scully, R. (2004). Control of sister chromatid recombination by histone H2AX. Mol. Cell *16*, 1017–1025.

Xiong, Y., Hannon, G. J., Zhang, H., Casso, D., Kobayashi, R., and Beach, D. (1993). p21 is a universal inhibitor of cyclin kinases. Nature *366*, 701–710.

Zachos, G., Rainey, M. D., and Gillespie, D. A. (2003). Chk1-deficient tumour cells are viable but exhibit multiple checkpoint and survival defects. EMBO J. *22*, 713–723.

Zhou, B.-B.S., and Elledge, S. J. (2000). The DNA damage response: putting checkpoints in perspective. Nature *408*, 433–439.

Zou, L., and Elledge, S. J. (2003). Sensing DNA damage through ATRIP recognition of RPA-ssDNA complexes. Science *300*, 1542–1548.